Mercury vertical and horizontal concentrations in agricultural soils of a historically contaminated site: Role of soil properties, chemical loading, and cultivated plant species in driving its mobility☆

Cristiana Morosini [a], Elisa Terzaghi [a], Giuseppe Raspa [b], Elisabetta Zanardini [a], Simone Anelli [c], Stefano Armiraglio [d], Elisa Petranich [e], Stefano Covelli [e], Antonio Di Guardo [a,*]

[a] DiSAT, University of Insubria, Via Valleggio 11, Como, Italy
[b] DICMA, Sapienza University of Rome, Via Eudossiana 18, Rome, Italy
[c] ERSAF, Via Pola 12, Milan, Italy
[d] Municipality of Brescia - Museum of Natural Sciences, Via Ozanam 4, Brescia, Italy
[e] Dept. of Mathematics & Geosciences, University of Trieste, Via E. Weiss 2, 34128, Trieste, Italy

A B S T R A C T

The long term vertical and horizontal mobility of mercury (Hg) in soils of agricultural areas of a historically contaminated Italian National Relevance Site (SIN Brescia-Caffaro) was investigated. The contamination resulted from the continuous discharge of Hg in irrigation waters by an industrial plant (Caffaro S.p.A), equipped with a mercury-cell chlor-alkali process. The contamination levels with depth ranged from about 20 mg/kg dry weight (d.w.) of soil in the top (plow) layer to less than 0.1 mg/kg d.w. at 1 m depth. The concentrations varied also spatially, up to one order of magnitude within the same field and showing a decreasing trend from the Hg source (i.e., irrigation ditches). The concentration profiles and gradients measured were explained considering Hg loading, soil properties, such as the texture, organic carbon content, pH and cation exchange capacity. A Selective Sequential Extraction (SSE) was also applied on soil samples from an *ad hoc* greenhouse experiment to investigate the role of different plant species in influencing Hg speciation in soils. Although most of the extracted Hg was included in scarcely mobile or immobile forms, some plant species (i.e., alfalfa) showed to importantly increase the soluble and exchangeable fractions with respect to the unplanted control soils, thus affecting mobility and potential bioavailability of Hg.

1. Introduction

Mercury (Hg) is a ubiquitous pollutant, that due to its persistent and bioaccumulative (e.g., methylmercury, CH_3Hg^+) properties, as well as its toxicity, can affect human health and ecosystems (Beckers and Rinklebe, 2017). The high volatility of some species, such as gaseous elemental mercury (GEM) and dimethylmercury ($(CH_3)_2Hg$), is also responsible for the potential long-range transport of this element, representing a global environmental threat (Gustin et al., 2020). Mercury in soil derives from natural sources (e.g., rock weathering, geothermal and volcanic emissions) and anthropogenic activities (e.g., mining, chlor-alkali industry, pesticide applications, solid waste incinerator, fossil fuel combustion) (Pirrone et al., 2010).

Mercury concentrations in soil could vary from less than 1 mg/kg (background levels) up to approximately 10,000 mg/kg in contaminated sites (Ottesen et al., 2013; Wang et al., 2012). More specifically, contaminated sites represent a sink for Hg, but soils could also act as a secondary source through volatilization to the atmosphere and infiltration to groundwaters. For this reason, an increasing number of recent studies focused on factors affecting Hg fate in order to determine the most effective remediation strategies for contaminated soils (Matsumoto and Liu, 2020; O'Connor et al., 2019; Yang et al., 2018). Mercury is strongly bound in soils to reduced sulphur groups and organic matter (Skyllberg et al., 2003). The equilibrium between sorption/desorption of Hg in soil depends on the presence and concentrations of several ions and compounds, such as S^-, Cl^- and dissolved organic carbon (DOC)

☆ This paper has been recommended for acceptance by Philip N. Smith.

* Corresponding author.
E-mail address: antonio.diguardo@uninsubria.it (A. Di Guardo).

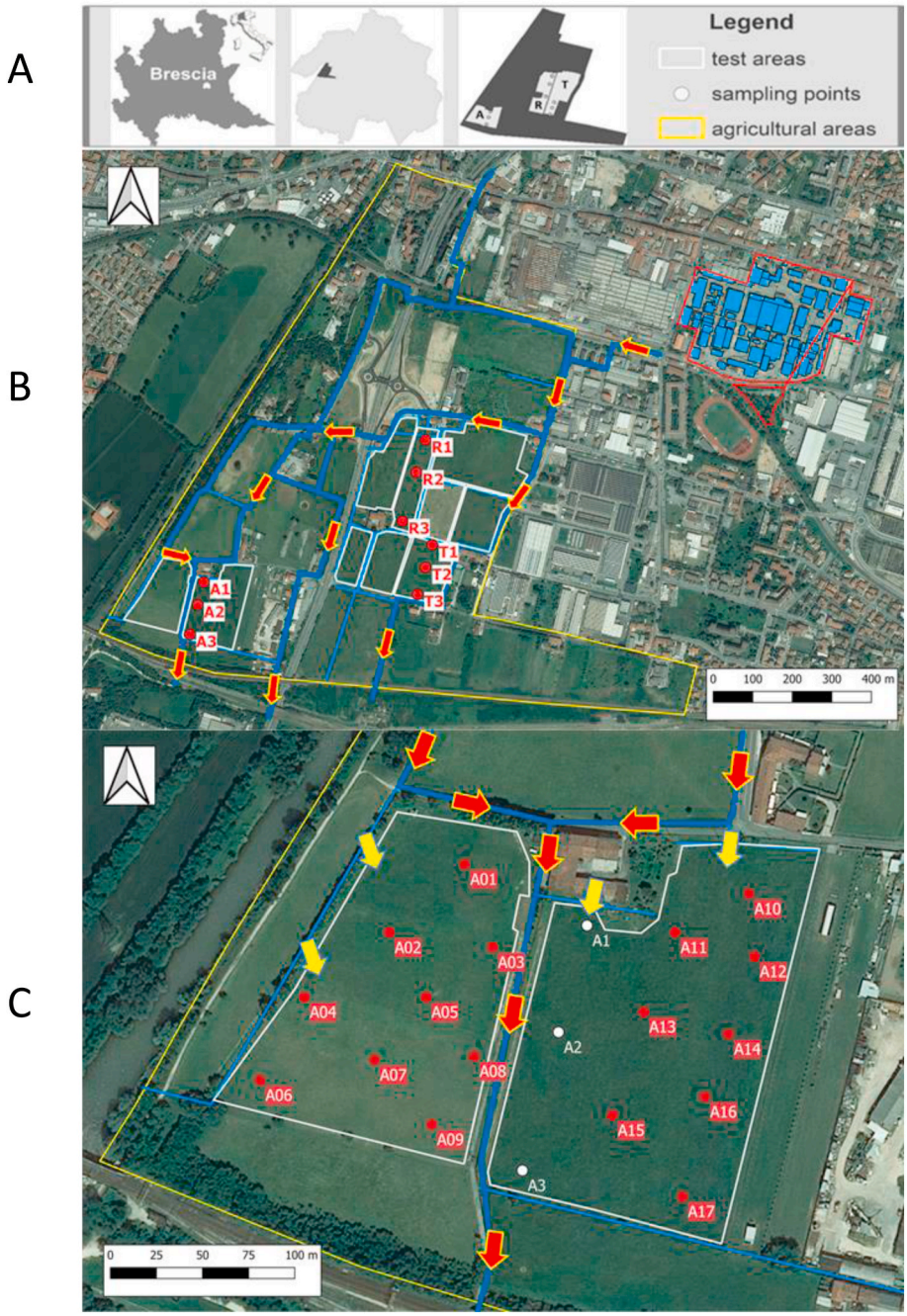

Fig. 1. Index map of the study area. Section A: From left to right: City of Brescia within Lombardy Region (dark grey) in Italy, contaminated agricultural fields included in the municipality area of Brescia (light grey), location of the sampling points (dark grey). Section B: The colored aerial pictures represent the fields sampled for the vertical soil profiles: area A (points A1, A2, and A3); area R (points R1, R2, and R3) and T (points T1, T2, and T3). The light blue area in the top right corner shows the location of the Caffaro Plant. The light blue lines represent the canal network and the red arrows the water direction. Section C: Area A: location of the additional sampling points (red dots) for the spatial analysis, including also the points of the soil profiles (white dots). The yellow arrows represent the surface irrigation water entry points. See the text for details. (For interpretation of the references to color in this figure legend, the reader is referred to the Web version of this article.)

(Gabriel and Williamson, 2004). The net evasion in its gaseous form is controlled by speciation, microbial activity, and by some other factors such as Fe^{2+}, and fulvic acids (Fritsche et al., 2008) and it is directly related to temperature rise and solar radiation intensity (Carpi and Lindberg, 1998; Kim et al., 2004).

In terms of fate and environmental distribution, Hg compounds can be divided in three main groups: elemental Hg (Hg(0)), its inorganic, and organic species (Matsumoto and Liu, 2020). Both inorganic and organic Hg could be present as several species, depending on texture, soil organic matter, DOC, ionic composition, oxygen level, pH, as well as microbial activities (Gabriel and Williamson, 2004). Among the inorganic Hg(II) species we can account HgS, $HgCl_2$, $HgSO_4$, HgO, whereas organic Hg(II) is represented by the methylated species (CH_3Hg^+ and $(CH_3)_2Hg$) (O'Connor et al., 2019). Mercury mobility, as well as its bioavailability, in soils is strictly associated to its chemical forms, therefore the measurement of total Hg concentration is not generally sufficient to fully evaluate Hg fate in soil and in the surrounding environmental media (air, water, biomass). For example, cinnabar (α-HgS) is among the most stable Hg form in soils, whereas CH_3Hg^+ can be bioaccumulated through the food web (Bavec and Gosar, 2016; Fernández-Martínez and Rucandio, 2014). For this reason, the use of sequential extraction procedures (Bloom et al., 2003) should be preferred as a specific approach to discriminate among the forms of Hg present in soils.

Hg can be found at relatively high concentrations in the soils of one of the most important contaminated sites of national relevance in Italy (SIN, *Sito d'Interesse Nazionale* in Italian) is the SIN Brescia-Caffaro, located in the city of Brescia (a city of about 200,000 inhabitants in northern Italy). The SIN was established in 2002 because of the contamination derived by the activities of the former Caffaro S.p.A. chemical factory, which produced an array of chlorinated chemicals,

including polychlorinated biphenyls (PCBs), between 1930 and 1984 (Di Guardo et al., 2017). The factory implemented the chlor-alkali process to obtain chlorine, from its early start, at the beginning of 1900, until 1997 (Ruzzenenti, 2001). This process used Hg cells and released metallic Hg into the wastewater stream, which ended up in a wide network of irrigation canals, for at least 90 years. These waters were used for irrigating different crops, thus affecting more than a hundred hectares of agricultural areas by a load of inorganics such as Hg and arsenic (As), as well as organics such as PCBs, dioxins and furans, at resulting levels often well above the regulatory thresholds for residential and agricultural land use. Many activities were undertaken to acquire a complete picture of the contamination to plan remediation actions (Bagnati et al., 2019; Di Guardo et al., 2020; Terzaghi et al., 2019, 2018a; 2018b; Vergani et al., 2017). Some of the previous activities and investigations by the local environmental authorities (Di Guardo et al., 2020) indicated that the elevated concentrations of contaminants in soil were due to the use of contaminated irrigation waters, with the highest levels in the top (plow) layer (40 cm) and in the northern points of the fields, close to the entry point of water (from the canals) used as surface irrigation.

In this work, Hg was measured in three different former agricultural areas of the SIN Brescia-Caffaro: the main objective was to evaluate the pattern and the factors involved in the vertical transfer of Hg down to 1 m depth and its further horizontal spreading in the whole field. Additionally, Hg fraction analysis was also conducted on soil samples collected from these fields and used in greenhouse experiments where different plant species were employed. The aim was to evaluate the influence of plant species in changing the ratio of Hg species present and, therefore, the potential change in mobility deriving by the cultivation of the different species on the same soil. The outcome of this work can also be useful to evaluate the conditions regulating the vertical transfer of Hg towards the surface aquifers, the potential for Hg volatilization as well as its bioaccumulation potential in the agricultural food chain. This knowledge will also be relevant when selecting and evaluating the phytoextraction-based remediation actions for Hg contaminated areas.

2. Materials and methods

2.1. Experimental sites and general features

Mercury was measured in three test areas (Areas A, R, and T, Fig. 1), part of a large agricultural territory just south west of the factory. Here cultivation was blocked by law in 2002, so the Hg input to soils. The sampling areas were chosen (Di Guardo et al., 2020) because of different crop history and soil use:

AREA A (5.1 ha): in this area meadows (also receiving winter irrigation since it was a water-meadow) and corn were the main crops.

AREA R (5.5 ha): this area was mostly characterized by crop rotation (e.g., clover, corn, and alfalfa).

AREA T (8.0 ha): this area was mostly cultivated with corn and alfalfa; some important soil leveling activities were undertaken because of field and canal rearrangement.Whereas these three areas were compared to evaluate the vertical distribution of Hg in different fields, only the area A was considered, as an example, to depict Hg horizontal spatial distribution.

2.2. Sampling strategy

2.2.1. Vertical distribution of Hg in soils

In each of area A, R, and T, Fig. 1, three sampling points were selected from North to South, along the (surface) irrigation path, (for a total of 9 points: A1, A2, A3; R1, R2, R3; T1, T2, and T3) (Di Guardo et al., 2020). Soil cores were taken in each point in October 2014, with a direct push mechanical dual tube sampling corer (Geoprobe DT7822), employing a 7.35 cm (3 inches) DT45 liner. The first sampling point of each field (i.e., A1, R1 and T1) was placed at a distance of about 11 m from the canal delivering the irrigation water (Table A1). Samples were obtained removing the grass cover on soil and coring the soil down to 1 m. Three replicated soil cores were taken for each of the 9 sampling points within 1 m (in total 27 cores). From each of the three replicated cores for each point, seven subsamples were obtained for 0–10 cm; 10–20 cm; 20–30 cm; 30–40 cm; 40–60 cm; 60–80 cm; 80–100 cm depths. Subsamples obtained from single cores gathered at the same depth interval were pooled *in situ* to obtain 63 homogenous composite samples in total. The intent of collecting three cores at each sampling points was to obtain a suitable local mean concentration value for each depth to prevent possible outliers from punctual concentrations.

2.2.2. Spatial gradient of Hg in soils

To investigate the spatial trend of Hg concentrations in Area A, 17 soil samples were collected (Fig. 1) in December 2014. Sampling was performed using the corer described above but coupled with a ~5 cm (2 inches) DT325 liner. In detail, for each point, 5 replicated samples (0–40 cm depth) were collected at the four vertices and in the center of a square of 1 m^2. The replicated samples were mixed and pooled *in situ* to obtain a homogenous sample.

Sampling and chemical analyses for the field sampling part of the study were performed by a commercial laboratory (Theolab S.p.A., now Mérieux NutriSciences, Volpiano TO, Italy).

2.3. Greenhouse experiment

To investigate the role of plant species in influencing Hg speciation and mobility in soil, a long-term (18 months) greenhouse experiment was performed using soil samples (0–40 cm depth) collected from Area R (Terzaghi et al., 2019). Four plant species i.e., *Festuca arundinacea* Schreb. (tall fescue), *Medicago sativa* L. (alfalfa), *Brassica juncea* (L.) Czern. (brown mustard), *Salix caprea* L. (goat willow) were employed. Ten seeds or one plant (i.e., for goat willow) were used for each species in polypropylene pots filled with about 6 kg of contaminated soil. An unplanted control soil was also set up. The experiment started in spring 2015 (T0), lasted for two consecutive growing seasons and ended in autumn 2016. Soil samples were collected twice in 2015 (T1 and T2) and in 2016 (T3 and T4) in summer and autumn. The samples were analyzed for total Hg at each sampling time, while Hg speciation was determined, at the beginning (T0) (unplanted control) and at the end of experiment (T4) (soil in which the 4 species were grown). The experiment was performed in triplicate, however, just one soil replicate was analyzed for Hg speciation. The greenhouse used in the experiment was not heated during the winter season to reflect the seasonal variability (min 10 °C in winter and max 40 °C in summer), while it was partially open during summer to avoid excessive temperature. The moisture level was maintained at about 30% of the soil total volume in all pots by drip irrigation. For a full description of the experiment please refer to a previous paper. (Terzaghi et al., 2019).

2.4. Chemical analyses

2.4.1. Field soil samples

Soil samples were prepared according to US-EPA 3051A Method (US EPA, 2007a). In brief, approximately 0.5 g of sample (air dried and sieved at 2 mm) were mineralized in a microwave digester (Ethos Touch Control-Milestone) with H_2O_2 (2 mL, 30%), HNO_3 (2 mL, 65%) and HCl (6 mL, 37%). After the digestion, samples were diluted to 500 mL with ultrapure water and were filtered to 0.45 μm pore size membrane filters (Millipore Millex-HA). Total Hg was measured according to US-EPA 6020A method (US EPA, 2007b) using an inductively coupled plasma-mass spectrometry, ICP-MS (Agilent, model 7500). The mass monitored were mass 201 and 202, while the mass used for quantitation was mass 202. The internal standard used was Lutetium. Three washing steps were carried out after each sample in order to minimize memory effects: a 4% mixture of nitric and hydrochloric acid, a 2% mixture of

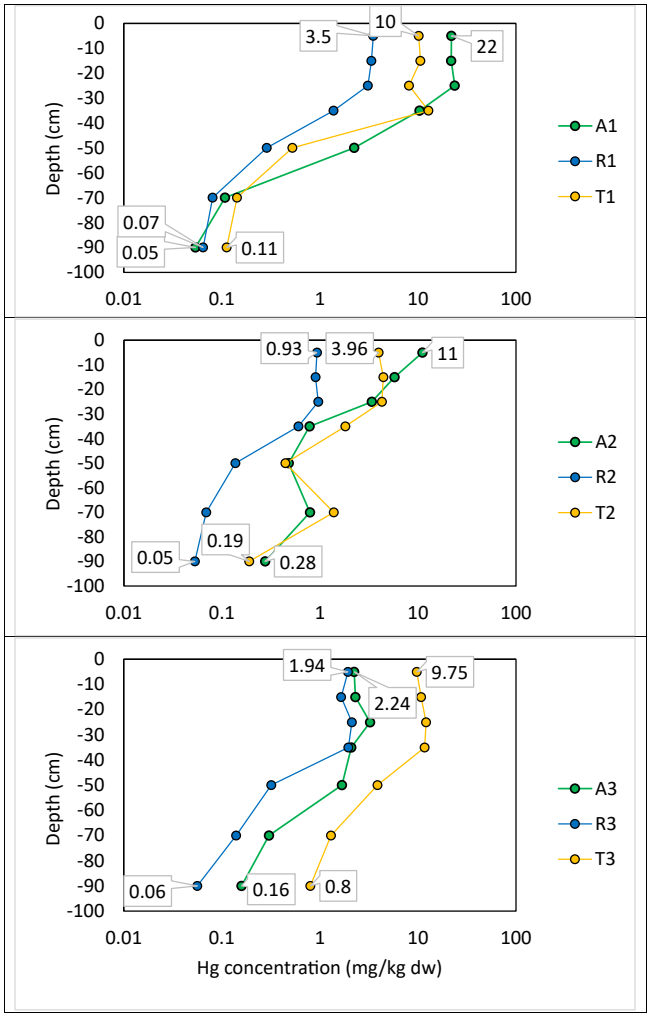

Fig. 2. Soil core profiles of total Hg concentrations in the three fields (A, R, and T) and in the corresponding three sampling points (1, 2 and 3) along each ideal North-South transect. Given the concentration log scale, the coefficients of variation could not be displayed. Please refer to Figure A3 instead.

ammonia and hydrogen peroxide and finally a 2% mixture of nitric and hydrochloric acid.

2.4.2. *Greenhouse soil samples*

The Selective Sequential Extraction (SSE) procedure (Bloom et al., 2003), subsequently adapted for sediments (Shi et al., 2005) was used for the soil samples of the greenhouse experiment. The five extractants used, at increasing extraction capacity, were: (1) Milli-Q water for "water-soluble Hg"; (2) CH_3COOH + HCl which aims at mimicking the bioaccessibility of Hg in the mammalian gastrointestinal tract; (3) KOH for "organo-chelated Hg"; (4) HNO_3 for "elemental/strongly complexed Hg" and (5) *aqua regia*, mainly for extracting insoluble species such as Hg sulphide (Table A2SI). An amount of ~0.4 g of lyophilized and fine-ground soil samples was placed into pre-conditioned borosilicate glass centrifuge tubes. Pre-conditioning was performed with a solution of 10% v/v Suprapure HCl (≥37%, VWR). The containers were heated at 50 °C for 12 h, rinsed with Milli-Q water and kept filled with the same water until samples were collected. After adding each selective extractant (V = 40 mL), the soil was shaken end-over-end for 18 ± 4 h at room temperature. The tubes were eventually centrifuged (3000 rpm; t = 20 min) and the supernatant was decanted and filtered through 0.45 μm pore size membrane filters (Millipore Millex-HA). The last fraction, F5, could not be filtered due to the extreme acidity of the solution. The five extracts were then placed in clear borosilicate bottles and oxidized using

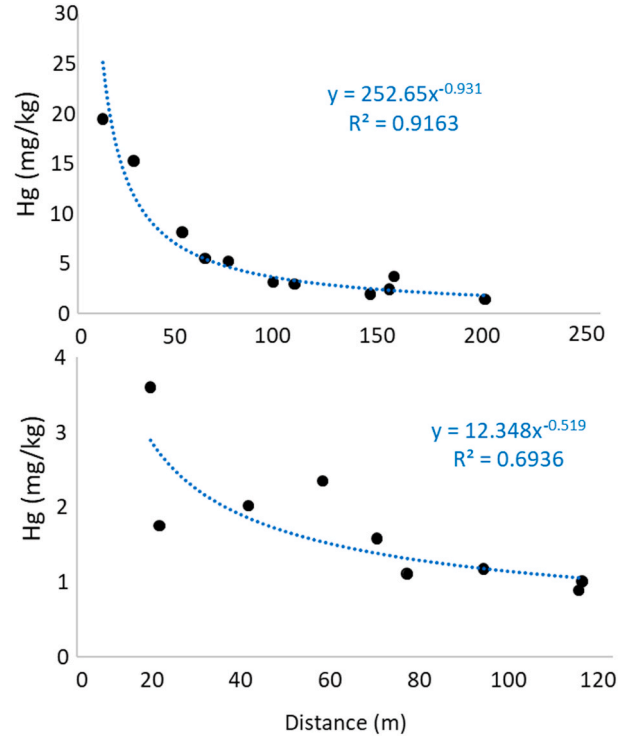

Fig. 3. Relationship between Hg concentrations in soil and the distance from the irrigation ditches (top: western field; bottom: eastern field) in Area A.

500 μL of BrCl. This was performed on all fractions, except for F3, which received 5 mL of BrCl, and F5 which did not receive the oxidant. The solid residue was then washed with the relative extractant and the resulting rinse was discarded. After the last step (F5), the deposit was air-dried and analyzed with a Direct Mercury Analyzer (DMA-80, Milestone) following the EPA Method 7473. Analyses of total dissolved Hg (DHg) in the extracted solutions obtained with SSE and in the filtered extractant solutions (employed as analytical blanks) were performed according to the EPA Method 1631e (US EPA, 2002) using AFS detection (Mercur, Analytic Jena) coupled with a gold trap pre-concentration system. A pre-reduction step with $SnCl_2$ 2% in HCl 4% was then completed after adding NH_2OH–HCl (30%, 0.25 mL) to the sample.

2.5. *QA/QC*

Field soil samples: Calibration curves were built in the range 0.2–5 mg/L, utilizing Hg analytical standard (Sigma Aldrich TraceCert 1000 mg/L in nitric acid) and external standard quantitation. LOQ was set as the lowest point in the calibration curve, 0.2 mg/L. Laboratory Control Samples (LCS) were used to monitor soil extraction (US EPA, 2007a) and recovery. Field and transport blanks were employed to monitor the potential contamination in the different phases, especially of the volatile species. These blanks, together with method blanks (analyzed at a ratio of 1 every 20 samples) were found to be at concentrations lower that 0.5 LOQ. NIST 2711A Montana II Soil was used as certified reference material for quality control. The recovery was 101.3% as average. Method detection limit (MDL) was calculated according (US EPA, 2016) and was 0.0329 mg/kg d.w. Measurement uncertainty was calculated according to (Horwitz et al., 1980). Method reproducibility was 3.91%.

Greenhouse soil samples: a NIST 3133 certified solution was used for method calibration while ORMS-5 (CRM, Canada) was used for quality control. The detection limit calculated, based on three times the standard deviations of ten reagent blank, was 0.63 ng/L while the quantification limit (LOQ), calculated based on ten times the standard deviations of ten reagent blank, was 2.11 ng/L. The method was verified

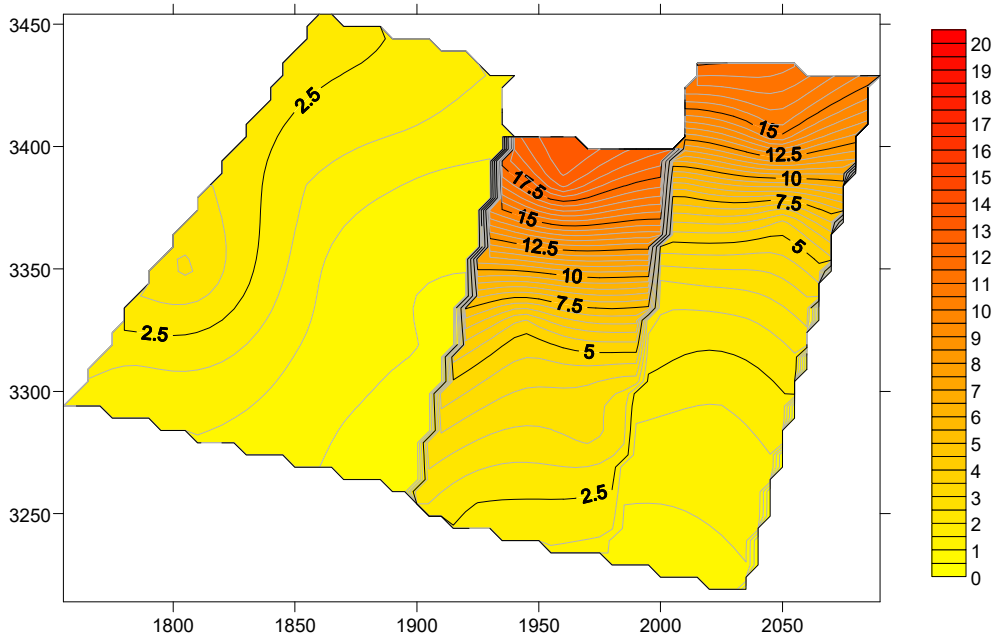

Fig. 4. Spatial variability of Hg concentrations (mg/kg) in topsoils of Area A.

by summing the fractions of extracted Hg in each phase (Hg_x) to total mercury (THg) in the sample (ΣHg_x/THg), where THg in the soil samples was in parallel measured with DMA-80. The average value of the ratios accounted for 0.89 ± 0.19. Method reproducibility was 4% and values were corrected for blanks.

2.6. Statistical analyses

Statistical analyses were performed using XLSTAT software (Addinsoft SARL, Version, 2021.1.1, Boston, USA). Principal component analysis (PCA) was used to compare different samples for Hg concentration and soil properties (texture, organic carbon, pH, cation exchange capacity) for each sampling point and depth. Regression analyses were employed to evaluate the trend of Hg concentration at increasing distance from the irrigation ditches. Correlation analysis was also performed to investigate the strength of the relationships between each soil properties and Hg concentrations in soil.

The spatial concentrations map for Area A was obtained using the intrinsic kriging method with automatic identification of the generalized covariance (Chilès and Delfiner, 2012). More details in the Appendix (Text A.1).

3. Results and discussion

3.1. Soil properties

Several soil properties (texture, organic carbon (OC) content, pH, and cation exchange capacity (CEC)) were measured in the core samples collected in the three fields at different depth, as reported in (Di Guardo et al., 2020) (Table A3and A4). The most typical textural class was sandy loam but some of the soils has larger sand and loam levels, classified as loamy sands (Maidment, 1993). Organic carbon showed a high variability among the agricultural fields, ranging from 0.34% to 3.81% in the plow layer (0–40 cm) and from 0.26% to 1.86% in the deepest soil layers (40–100 cm). Similarly, CEC generally dropped from top to bottom (i.e., on average from 21.7 ± 3.1 meq/100g (0–40 cm) to 16.6 ± 3.3 meq/100g (40–100 cm)). pH was neutral/alkaline, varying between 7.02 and 8.76 throughout all fields and sampling depth.

3.2. Mercury concentrations in soil: origin of the contamination and comparison with other sites

The continuous release of unknown quantities of elemental Hg(0) and inorganic Hg(II) species as effluents from the Brescia-Caffaro chlor-alkali plant into the irrigation canals determined a slow and gradual accumulation (in an estimated period of about 90 years) of Hg in soils of the nearby agricultural fields. During irrigation events, Hg contaminated waters were directed from the ditches into the fields, generally from the North side of the area (see Fig. 1 and A2SI) (Di Guardo et al., 2020). The highest Hg concentrations at the entry points and the length of the water to soil path (both vertically and horizontally), together with the relative permeability of the soil, have determined a characteristic vertical and horizontal distribution of Hg in the soil matrix.

Total Hg concentrations, reported as dry weight, in the superficial soil (0–20 cm) fall between 0.9 and 22 mg/kg (Table A3 SI). These values are generally well above the legal threshold for agricultural soils in Italy, which is 1 mg/kg (Italian MEPS, 2019) and are considerably higher than the median values for agricultural and grazing land soils (0–20 cm) (0.030–0.035 mg/kg) reported from a recent survey on the "background" European soils (Ottesen et al., 2013). In this survey, where more than 4000 samples were analyzed, the maximum values vary between 1.6 and 3.1 mg/kg, just bordering the minimum values found in the contaminated site SIN Brescia-Caffaro. In the same study, a geochemical map, representing Hg concentration values for agricultural soils in Europe, reports Hg contents from 0.0183 to 0.0476 mg/kg as representative concentrations for the expected background in Northern Italy (Ottesen et al., 2013). These values are well below the range of concentrations found in the topsoil of our study areas, which are from about 50 to 460 times higher. Mercury concentrations in the SIN Brescia-Caffaro are close to those reported for other chlor-alkali plant contaminated soils (e.g., 0.1–91 mg/kg), generally lower than the concentrations found in soils contaminated by Hg mining activities (i.e., from hundreds to thousands mg/kg) (Wang et al., 2012). Several other studies can be found reporting Hg contamination of agricultural soils derived by several industrial plants, such as acetaldehyde-producing companies in Switzerland (Gilli et al., 2018; Gygax et al., 2019), several industrial activities in China (Luo et al., 2008), Spain (Reis et al., 2009), the Netherlands (Bernaus et al., 2006), Germany (Rinklebe et al., 2010).

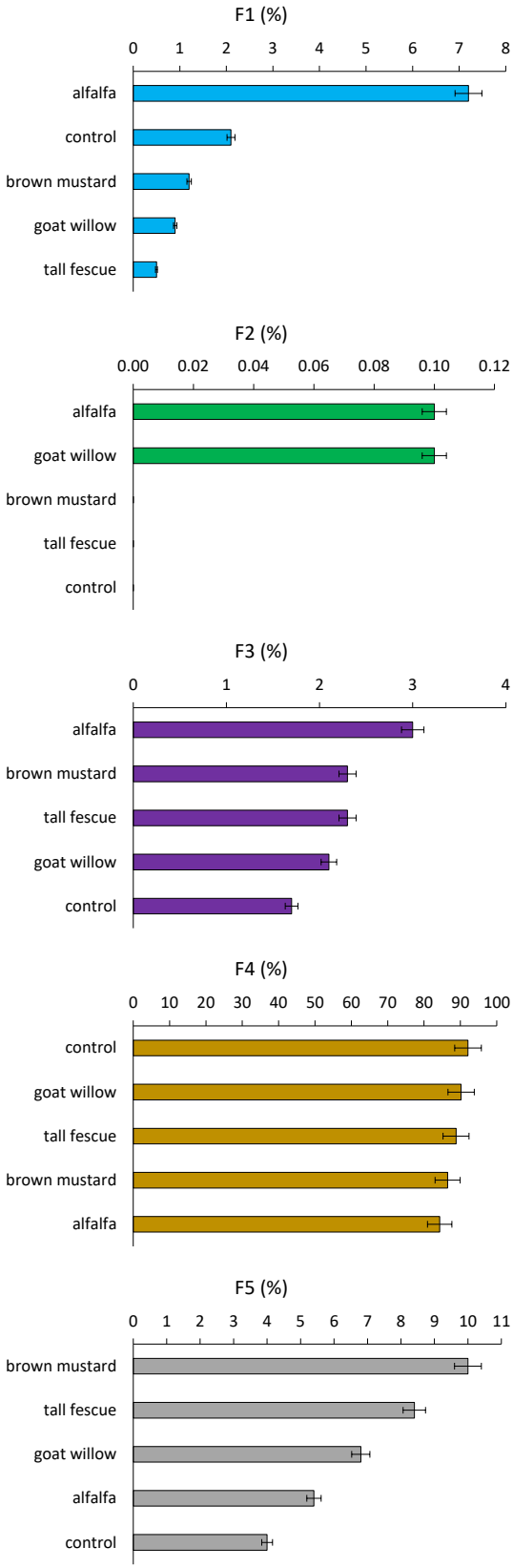

Fig. 5. Ranking of plant species and unplanted control soil samples according to the percentage of the Hg fractions obtained from selective extraction procedure on the total soil sample. Error bars represent the coefficient of variation.

3.3. Mercury concentrations in soil profiles

Two general patterns appear when focusing on Hg concentrations in soil profiles of the three areas (Fig. 2 and A3). Area A is the most contaminated area, showing Hg average concentrations of about 20 mg/kg in the plow layer in point A1, about 2–7 times the concentrations of T1 and R1. This can be due to a higher use of irrigation water, since in this part of the field a water meadow was present, receiving irrigation also in winter, to guarantee higher grass production. Moreover, the largest Hg concentrations in all sampling points are generally observed within the first 40 cm of the soil profile and in point 1 for all areas, close to the irrigation inlet. Concentrations are nearly homogeneous in the first 30–40 cm, due to the plowing activities, the input of Hg from top due to irrigation and the general higher OC content in topsoils. Similar patterns of concentration decrease with depth were obtained for soils contaminated with mercuric nitrate and metallic Hg (Revis et al., 1989), in a land treatment system which were irrigated with municipal wastewaters (Yediler et al., 1994), as well as in an industrial area in China which received elemental Hg spills (Zhang et al., 2018). In soil core profiles, Hg concentrations dropped sharply at increasing depth. At 100 cm depth, concentrations are up to 3 orders of magnitude lower than in the topsoil layers.

Similar behaviour with depth was obtained on the same area when evaluating PCBs (Di Guardo et al., 2020), which were also present in the irrigation waters and discharged jointly with Hg, although for a shorter time interval. PCA identified that about 90% of the variance for 7 variables (Hg concentrations and soil properties) was explained by 4 components (F). The results suggest a different pattern among the three fields, and 63% of the variance was described by the first two principal components. The relationships among the variables and the samples are shown in the biplot (Figure A1 SI). The most important variables associated with the first component are CEC, OC, and Hg concentrations, which are inversely correlated to pH. The variables that characterized the second component are silt and clay which are inversely correlated. Therefore, whereas the second component divides samples according to their texture (sandy vs loamy soil), the first component explains the separation among the samples due to their Hg concentrations and the variability of the other soil parameters (OC, CEC and pH). In general, samples of each field belong to three separate clusters according to their texture. Moreover, within each cluster, points representing upper layers are clearly separated from those points related to deep layers on first component, thus indicating there is a gradient of Hg concentrations, OC and CEC with depth. Whereas samples from A and R areas intersect together, indicating common behaviour and features, the T area samples cluster in a different part of the chart. This can be also due to the soil levelling activities, which occurred in area T, and might have altered the concentrations in the soil profile.

To better evaluate the relationships between the different variables included in the PCA (i.e., soil properties and Hg concentration) a correlation analysis was performed considering the 3 points of field A. While significant correlations were not found between Hg concentrations and soil properties in point A2, Hg concentrations are significantly ($\alpha = 0.05$) correlated to depth ($\rho = -0.896$) and OC ($\rho = 0.995$) in A1 and to depth ($\rho = -0.995$), silt ($\rho = 0.960$), sand ($\rho = -0.957$), pH ($\rho = -0.969$) and CEC ($\rho = 0.995$) in A3 (Tables A5-A7 SI). In fact, many authors report that the behaviour of Hg with depth can be influenced by the presence of organic matter, clays and other mineral components such as oxyhydroxides of Fe and Mn (Bernaus et al., 2006; Palmieri et al., 2006), as well as texture, DOC and the redox potential, especially in frequently flooded soils (Beckers and Rinklebe, 2017).

3.4. Spatial variability of Hg concentration in field A

When evaluating spatial variability of concentrations in topsoil, one should consider the path from the source of contamination (i.e., the inlet in the field of contaminated irrigation water of the ditch network) (Fig. 1

and A2 SI) and the travel distance of water during the irrigation events. Regression analysis of concentrations in topsoil vs. distance from the inlet (Table A4) shows a good fit both for the eastern field points (R^2 = 0.91) and western field points (R^2 = 0.70) (Fig. 3). This indicates a progressive Hg depletion of irrigation water, while flowing over land to the end of the field. The distance by which concentrations in soil decreased by half is about 40 m, showing a gentler decrease with distance in the remaining path. The concentrations close to the inlet are much higher in the eastern field by a factor of 3–10 and so is the decrease with distance. This might indicate a different discharge rate of Hg from the irrigation ditches due to a variable concentration of Hg in water and/or an unlike irrigation times and, therefore, amount of water used. It can be justified by the fact that the eastern field of Area A was cultivated with water meadows and corn, which required frequent irrigation water at maturity growth stages.

To assess the spatial distribution of mercury in the topsoil with the intrinsic kriging method a realignment of the emission points from the irrigation canals in the north part of the eastern plot in Area A (Fig. 1 C) was necessary to correctly perform the spatial correlations. This was due to the dependence of the concentration gradient on the distance of the canals on the one hand and the misalignment of the two canals of the eastern field on the other. For this reason, the coordinates of the points sampled on the left side of the eastern field (points A1 to A3) were virtually moved upwards by 40 m in the direction of the water flow to ideally realign the two edges of the eastern field. Once the concentrations were estimated, the nodes of the grid (estimation) located in the same part of the field, were moved in the opposite direction by the same amount, before calculating the isolines. The resulting concentration map (Fig. 4) shows mercury concentrations in the surface soil samples (0–40 cm) of field A, which varied of two orders of magnitude ranging from 0.9 to 19.5 mg/kg (Table A3 and A4 SI).

The highest contents were measured in the top eastern and middle parts of the area, whereas, in the western part, concentrations were more homogeneous. Moreover, as outlined above a decreasing trend of Hg concentrations at increasing distance from the irrigation ditches can be observed from a spatial perspective as well. This seems to indicate that the factors involved in the spatial spreading of Hg in the plow layer are mostly physical, related to the surface water irrigation movement and its Hg depletion with distance (Fig. 3) due to the soil water retention and Hg adsorption (depending on organic carbon, texture, etc.), and to the soil mixing activities (plowing and tillage, etc.).

We could not find similar detailed studies of Hg spatial distribution in the literature: most of spatial maps in surface soils were obtained at much larger scale, such as in an area of 1600 ha in Serbia, with units of 4 × 4 km and samples taken at the center of this quadrant (Ninkov et al., 2017) or in the north of Pearl River Delta, (China), where 104 topsoil samples were taken in a region of more than 600,000 ha (Jiang et al., 2019) or a similarly sized region in Colombia (Marrugo-Negrete et al., 2019). A somehow similar situation of a chloro alkali plant derived contamination was that recently depicted for mangrove soil area in Brazil (Araújo et al., 2021). In this study Hg was found, after an historical release, in sediment and water of River Botafoco, affecting the adjacent Mangrove soils, with concentrations up to 14.4 mg/kg. In this study the authors also observed a decline of Hg concentration with distance, although up to several km.

3.5. Mercury fractions in soil

The results obtained from the SSE performed on greenhouse soil samples showed that the F1 and F2 fractions, the most soluble, generally represented a small percentage of the total Hg extracted (0.5–2.1%) (Table A8 SI and Fig. 5). However, in the alfalfa soil sample the percentage of Hg extracted from water (F1) was about 7%, much larger (by a factor of 3–14) than in the soil of the other plant species and the unplanted control sample. This could indicate a specific effect of alfalfa rhizosphere in mobilizing Hg in soils. The fraction F3, representative of the Hg bound to the organic matter, especially to humic acids, was found in levels which were always larger than the first two fractions, F1 and F2, except in the unplanted control sample (F3 = 1.7%) and alfalfa (F3 = 3.0%). The most abundant fraction was F4 (elemental/strongly complexed Hg) ranging from 84% to 92%. Fraction F5, corresponding to immobile Hg sulphides, mainly metacinnabar (β-HgS), varied from 4% to 10%. The largest values corresponded to brown mustard and tall fescue, although all the plant species seemed to be able to increase this immobile fraction of Hg, comparing to the control soil sample. Therefore, although most of the extracted Hg was actually included in F4, some plant species seem to increase (i.e., alfalfa) or reduce (i.e., brown mustard and tall fescue) Hg mobility better than other treatments and the unplanted control soil sample (Fig. 5).

The F1 and F2 fractions represent the most soluble compounds of Hg, most mobile and easily exchangeable from soils. The sum of the F1 and F2 fractions can be considered a good indicator of the fraction of Hg potentially accessible to organisms and in particular to bacteria capable of transforming the inorganic forms into methylmercury, more toxic and easily accumulated along the trophic chain (Bloom et al., 2003; Issaro et al., 2009; Shi et al., 2005). The F3 fraction, representing Hg bound to organic matter and humic acids, is not abundant in these soils. Although the mobility of this species is lower than those belonging to the F1 and F2 fractions, the extracted amounts were larger than F2, especially for alfalfa. A similar fingerprint was found in some samples from a study performed in the vicinity of a chlor-alkali plant in Tuzla, Bosnia and Herzegovina (Huremović et al., 2017). Several authors (Bloom et al., 2003; Fernández-Martínez and Rucandio, 2014) reported that F3 is likely the fraction most correlated with the methylation potential. The sum of F4 and F5 fractions, totaling altogether approximately 95% of the extracted Hg, suggests that the mobility of Hg from these soils is significantly reduced, given the negligible solubility of Hg associated with these fractions (Ravichandran, 2004).

Few studies investigated the role of plant species in influencing Hg fractions in soil. For example, in a greenhouse experiment performed with a heavily contaminated soil cultivated with *Chenopodium glaucum* L. (Wang et al., 2011), this species significantly increased, after 60 days, the soluble and exchangeable fractions of Hg up to one order of magnitude with respect to the unplanted control, while it nearly halved the oxide bound fractions; the organic bound fraction and the residual fractions were not significantly affected. The observed variations demonstrated that this plant species during its growth could change the ratio of Hg species in soil, likely due to the release of root exudates. These compounds were shown to be relevant against heavy metal stress (Montiel-Rozas et al., 2016), having also an impact on metal bioavailability in soil (Kim et al., 2010). Additionally, it was shown (Montiel-Rozas et al., 2016) that *Medicago polymorpha* L., a plant species of the same genus of alfalfa, was the species (in an experiment in which also *Poa annua* L. and *Malva sylvestris* L. were evaluated) which released the largest amounts of root exudates (such as low molecular weight organic acids, especially oxalic and malic acids, and to a limited extent citric and fumaric acids) as a defense mechanism, allowing the plant to reduce the uptake and grow at higher level of heavy metal contamination. These findings can justify the higher levels of F1, F2 and F3 Hg fractions shown in Fig. 5 for alfalfa.

Other authors (Yin et al., 2016) investigated Hg speciation in relation to cultivation practices, comparing rice and corn land cropping soil samples. Although the predominant Hg forms was β-HgS, minor amounts of the most bioavailable forms (i.e., $HgCl_2$ and Hg(0)) were also detected in both types of soil. A recent study (Gui et al., 2020) showed that Hg bioavailable fractions in soil increased (from 20% to 40%) during the 10 years of cultivation of a *Phyllostachys praecox* (bamboo) stand.

3.6. Mobility of Hg in soil: groundwater vs. atmosphere pathways

Although most of Hg seems to be confined in the top (plow) layer and

in those areas close to the irrigation inlets (Figs. 2 and 4), the continuous supply of Hg with time in association with the irrigation water produced a sort of steady progression of Hg accumulation with depth. The concentration difference between the plow layer and the bottom layer, at 1 m depth, is generally of about one to two orders of magnitude, much lower, for example, than the difference, in the same fields and conditions of total PCBs (Di Guardo et al., 2020), which was between two and three orders of magnitude. This means that the vertical mobility of mercury is significantly higher than that of PCBs, possibly also influenced by similar factors which were shown to enhance vertical PCB mobility. Among these factors there is DOC, acting as cosolvent and carrier towards the deepest layers, as also observed for Illinois soils (Dreher and Follmer, 2004); however, in presence of DOC, ionic Hg can also be photochemically reduced to elemental Hg, which may eventually volatilize (Ravichandran, 2004). Additionally, it should be also considered that in the SIN Brescia-Caffaro fields the sand and silt fractions increase with depth (Table A3), thus enhancing soil permeability and favoring the vertical movement through percolation of Hg soluble fractions and/or Hg bound to fine particles. Also, volatile species could be lost towards the atmosphere, considering the large percentage of the F4 fraction which also includes elemental Hg, and the possible interspecies conversion versus the F3 fraction, considered the precursor of methylated volatile species (Bloom et al., 2003). GEM was in fact shown to volatilize from these soils and a specific measurement campaign was carried out in Area A. Details on these volatilization fluxes are presented in a companion paper (Quant et al., 2021). The presence of vegetation, in this respect, could act stabilizing Hg as sulphide (F5) forms (as it appears from Fig. 5). It could also increase its mobility, either vertical or horizontal, as it appears with the soil in which alfalfa was cultivated. Although some modelling attempts to predict long term Hg fate in soil are available (Letermeand Jacques, 2015; Tsiros and Ambrose, 1999), further studies are needed to better account for the influence of vegetation on the mass balance of Hg in agricultural soils.

4. Conclusions

The continuous historical supply of Hg to agricultural soils in the SIN Brescia Caffaro offered a very important example to study the long term vertical and horizontal mobility of Hg in soil. The results show that Hg is capable to move to 1 m depth (and possibly beyond) at appreciable concentrations. The spatial analyses, investigating horizontal and vertical mobility, permitted to evaluate how the distribution in the plow layer and beyond was influenced by chemical loading, water movement, crop type, soil characteristics, as well as soil levelling activities. SSE analysis showed that nearly all Hg is in relatively immobile fractions (F4 and F5). The greenhouse experiment conducted with the same soil of the studied areas allowed to determine the potential influence of crop type on the fractions of Hg is soil, enhancing or slowing down potential losses towards groundwater or to the atmosphere. Although more work is necessary to fully assess the role of vegetation and its rhizosphere in mobilizing vs. immobilizing Hg in soil, especially evaluating this effect in time, it already provided precious information to plan future studies of rhizoremediation in this and other contexts.

Credit author statement

The authors have all equally contributed to the manuscript preparation and finalization.

Declaration of competing interest

The authors declare that they have no known competing financial interests or personal relationships that could have appeared to influence the work reported in this paper.

Acknowledgements

The authors would like to acknowledge their coworkers in the project, funded by Ente Regionale per i Servizi all'Agricoltura e alle Foreste (ERSAF), Lombardy Region, Italy, Decreto ERSAF n. III/5426 of December 09, 2013 and in particular Sara Borin, Francesca Mapelli, Lorenzo Vergani (University of Milan), Paolo Nastasio, and Vanna Maria Sale (ERSAF). The Department of Science and High Technology of the University of Insubria is kindly acknowledged for funding part of the salary of E.T.

Appendix A. Supplementary data

Supplementary data to this article can be found online at https://doi.org/10.1016/j.envpol.2021.117467.

References

Araújo, P.R.M., Biondi, C.M., do Nascimento, C.W.A., da Silva, F.B.V., da Silva, W.R., da Silva, F.L., de Melo Ferreira, D.K., 2021. Assessing the spatial distribution and ecologic and human health risks in mangrove soils polluted by Hg in northeastern Brazil. Chemosphere 266, 129019. https://doi.org/10.1016/j.chemosphere.2020.129019.

Bagnati, R., Terzaghi, E., Passoni, A., Davoli, E., Fattore, E., Maspero, A., Palmisano, G., Zanardini, E., Borin, S., Di Guardo, A., 2019. Identification of sulfonated and hydroxy-sulfonated PCB metabolites in soil: new classes of intermediate products of PCB degradation? Environ. Sci. Technol. https://doi.org/10.1021/acs.est.9b03010.

Bavec, Š., Gosar, M., 2016. Speciation, mobility and bioaccessibility of Hg in the polluted urban soil of Idrija (Slovenia). Geoderma 273, 115–130. https://doi.org/10.1016/j.geoderma.2016.03.015.

Beckers, F., Rinklebe, J., 2017. Cycling of mercury in the environment: sources, fate, and human health implications: a review. Crit. Rev. Environ. Sci. Technol. 47, 693–794. https://doi.org/10.1080/10643389.2017.1326277.

Bernaus, A., Gaona, X., van Ree, D., Valiente, M., 2006. Determination of mercury in polluted soils surrounding a chlor-alkali plant: direct speciation by X-ray absorption spectroscopy techniques and preliminary geochemical characterisation of the area. Anal. Chim. Acta 565, 73–80. https://doi.org/10.1016/j.aca.2006.02.020.

Bloom, N.S., Preus, E., Katon, J., Hiltner, M., 2003. Selective extractions to assess the biogeochemically relevant fractionation of inorganic mercury in sediments and soils. Anal. Chim. Acta 479, 233–248. https://doi.org/10.1016/S0003-2670(02)01550-7.

Carpi, A., Lindberg, S.E., 1998. Application of a teflon^{TM} dynamic flux chamber for quantifying soil mercury flux: tests and results over background soil. Atmos. Environ. 32, 873–882. https://doi.org/10.1016/S1352-2310(97)00133-7.

Chilès, J.-P., Delfiner, P., 2012. Geostatistics: Modeling Spatial Uncertainty, second ed. Wiley series in probability and statistics. Wiley, Hoboken, N.J.

Di Guardo, A., Raspa, G., Terzaghi, E., Vergani, L., Mapelli, F., Borin, S., Zanardini, E., Morosini, C., Anelli, S., Nastasio, P., Sale, V.M., Armiraglio, S., 2020. PCB vertical and horizontal movement in agricultural soils of a highly contaminated site: role of soil properties, cultivation history and PCB physico-chemical parameters. Sci. Total Environ. 747, 141477. https://doi.org/10.1016/j.scitotenv.2020.141477.

Di Guardo, A., Terzaghi, E., Raspa, G., Borin, S., Mapelli, F., Chouaia, B., Zanardini, E., Morosini, C., Colombo, A., Fattore, E., Davoli, E., Armiraglio, S., Sale, V.M., Anelli, S., Nastasio, P., 2017. Differentiating current and past PCB and PCDD/F sources: the role of a large contaminated soil site in an industrialized city area. Environ. Pollut. https://doi.org/10.1016/j.envpol.2017.01.033.

Dreher, G.B., Follmer, L.R., 2004. Mercury content of Illinois soils. Water. Air. Soil Pollut 156, 299–315. https://doi.org/10.1023/B:WATE.0000036824.07207.16.

Fernández-Martínez, R., Rucandio, I., 2014. Total mercury, organic mercury and mercury fractionation in soil profiles from the Almadén mercury mine area. Environ. Sci. Process. Impacts 16, 333. https://doi.org/10.1039/c3em00445g.

Fritsche, J., Obrist, D., Alewell, C., 2008. Evidence of microbial control of Hg0 emissions from uncontaminated terrestrial soils. J. Plant Nutr. Soil Sci. 171, 200–209. https://doi.org/10.1002/jpln.200625211.

Gabriel, M.C., Williamson, D.G., 2004. Principal biogeochemical factors affecting the speciation and transport of mercury through the terrestrial environment. Environ. Geochem. Health 26, 421–434. https://doi.org/10.1007/s10653-004-1308-0.

Gilli, R.S., Karlen, C., Weber, M., Rüegg, J., Barmettler, K., Biester, H., Boivin, P., Kretzschmar, R., 2018. Speciation and Mobility of Mercury in Soils Contaminated by Legacy Emissions from a Chemical Factory in the Rhône Valley in Canton of Valais, Switzerland, vol. 22.

Gui, R., Hu, Y., Li, Q., Zhuang, S., 2020. Effect of cultivation time on soil heavy metal accumulation and bioavailability in Phyllostachys praecox stands. Pedosphere 30, 810–816. https://doi.org/10.1016/S1002-0160(20)60033-9.

Gustin, M.S., Bank, M.S., Bishop, K., Bowman, K., Branfireun, B., Chételat, J., Eckley, C. S., Hammerschmidt, C.R., Lamborg, C., Lyman, S., Martínez-Cortizas, A., Sommar, J., Tsui, M.T.-K., Zhang, T., 2020. Mercury biogeochemical cycling: a synthesis of recent scientific advances. Sci. Total Environ. 737, 139619. https://doi.org/10.1016/j.scitotenv.2020.139619.

Gygax, S., Gfeller, L., Wilcke, W., Mestrot, A., 2019. Emerging investigator series: mercury mobility and methylmercury formation in a contaminated agricultural flood

plain: influence of flooding and manure addition. Environ. Sci. Process. Impacts 21. https://doi.org/10.1039/C9EM00257J, 2008–2019.
Horwitz, W., Kamps, L.V.R., Boyer, K.W., 1980. Quality assurance in the analysis of foods for trace constituents. J. AOAC Int. 63, 1344–1354. https://doi.org/10.1093/jaoac/63.6.1344.
Huremović, J., Horvat, M., Kotnik, J., Kocman, D., Žižek, S., Guevara, S.R., Muhić-Šarac, T., Memić, M., 2017. Characterization of mercury contamination surrounding a chloralkali production facility in Tuzla, Bosnia and Herzegovina. Anal. Lett. 50, 1049–1064. https://doi.org/10.1080/00032719.2016.1205595.
Issaro, N., Abi-Ghanem, C., Bermond, A., 2009. Fractionation studies of mercury in soils and sediments: a review of the chemical reagents used for mercury extraction. Anal. Chim. Acta 631, 1–12. https://doi.org/10.1016/j.aca.2008.10.020.
Italian, M.E.P.S., 2019. Italian ministry of the environment and the protection of the territory and the sea). In: Regulation Relating to Remediation and Restoration Interventions Environmental and Safety, Emergency, Operational and Permanent, of the Areas Destined for Production Agricultural and Livestock Farming, Pursuant to Article 241 of the Decree Legislative 3 April 2006, p. 152.
Jiang, X., Zou, B., Feng, H., Tang, J., Tu, Y., Zhao, X., 2019. Spatial distribution mapping of Hg contamination in subclass agricultural soils using GIS enhanced multiple linear regression. J. Geochem. Explor. 196, 1–7. https://doi.org/10.1016/j.gexplo.2018.10.002.
Kim, C.S., Rytuba, J.J., Brown, G.E., 2004. Geological and anthropogenic factors influencing mercury speciation in mine wastes: an EXAFS spectroscopy study. Appl. Geochem. 19, 379–393. https://doi.org/10.1016/S0883-2927(03)00147-1.
Kim, K.R., Owens, G., Naidu, R., 2010. Effect of root-induced chemical changes on dynamics and plant uptake of heavy metals in rhizosphere soils. Pedosphere 20, 494–504. https://doi.org/10.1016/S1002-0160(10)60039-2.
Leterme, B., Jacques, D., 2015. A reactive transport model for mercury fate in contaminated soil—sensitivity analysis. Environ. Sci. Pollut. Res. 22, 16830–16842. https://doi.org/10.1007/s11356-015-4876-x.
Luo, W., Lu, Y., Wang, B., Tong, X., Wang, G., Shi, Y., Wang, T., Giesy, J.P., 2008. Distribution and sources of mercury in soils from former industrialized urban areas of Beijing, China. Environ. Monit. Assess. 158, 507. https://doi.org/10.1007/s10661-008-0600-3.
Maidment, D.R. (Ed.), 1993. Handbook of Hydrology. McGraw-Hill, New York.
Marrugo-Negrete, J., Pinedo-Hernández, J., Combatt, E.M., Bravo, A.G., Díez, S., 2019. Flood-induced metal contamination in the topsoil of floodplain agricultural soils: a case-study in Colombia. Land Degrad. Dev. 30, 2139–2149. https://doi.org/10.1002/ldr.3398.
Matsumoto, M., Liu, H., 2020. Mercury speciation and remediation strategies at a historically elemental mercury spilled site. J. Hazard Mater. 384, 121351. https://doi.org/10.1016/j.jhazmat.2019.121351.
Montiel-Rozas, M.M., Madejón, E., Madejón, P., 2016. Effect of heavy metals and organic matter on root exudates (low molecular weight organic acids) of herbaceous species: an assessment in sand and soil conditions under different levels of contamination. Environ. Pollut. 216, 273–281. https://doi.org/10.1016/j.envpol.2016.05.080.
Ninkov, J., Marković, S., Banjac, D., Vasin, J., Milić, S., Banjac, B., Mihailović, A., 2017. Mercury content in agricultural soils (Vojvodina Province, Serbia). Environ. Sci. Pollut. Res. 24, 10966–10975. https://doi.org/10.1007/s11356-016-7897-1.
O'Connor, D., Hou, D., Ok, Y.S., Mulder, J., Duan, L., Wu, Q., Wang, S., Tack, F.M.G., Rinklebe, J., 2019. Mercury speciation, transformation, and transportation in soils, atmospheric flux, and implications for risk management: a critical review. Environ. Int. 126, 747–761. https://doi.org/10.1016/j.envint.2019.03.019.
Ottesen, R.T., Birke, M., Finne, T.E., Gosar, M., Locutura, J., Reimann, C., Tarvainen, T., 2013. Mercury in European agricultural and grazing land soils. Appl. Geochem. 33, 1–12. https://doi.org/10.1016/j.apgeochem.2012.12.013.
Palmieri, H.E.L., Nalini, H.A., Leonel, L.V., Windmöller, C.C., Santos, R.C., de Brito, W., 2006. Quantification and speciation of mercury in soils from the tripuí ecological station, minas gerais, Brazil. In: Sci. Total Environ., Selected Papers from the 7th International Conference on Mercury as a Global Pollutant, Ljubljana, Slovenia June 27 - July 2, 2004 368, pp. 69–78. https://doi.org/10.1016/j.scitotenv.2005.09.085.
Pirrone, N., Cinnirella, S., Feng, X., Finkelman, R.B., Friedli, H.R., Leaner, J., Mason, R., Mukherjee, A.B., Stracher, G.B., Streets, D.G., Telmer, K., 2010. Global mercury emissions to the atmosphere from anthropogenic and natural sources (preprint). In: Gases/Atmospheric Modelling/Troposphere/Chemistry (Chemical Composition and Reactions). https://doi.org/10.5194/acpd-10-4719-2010.
Quant, I.M., Feigis, M., Shreya, M., Lei, Y.D., Mitchell, C.P.J., Staebler, R., Di Guardo, A., Terzaghi, E., Wania, F., 2021. Using passive air samplers to quantify vertical gaseous elemental mercury concentration gradients within a forest and above soil. Submitt. J. Geophys. Res. Atmospheres.
Ravichandran, M., 2004. Interactions between mercury and dissolved organic matter—a review. Chemosphere 55, 319–331. https://doi.org/10.1016/j.chemosphere.2003.11.011.
Reis, A.T., Rodrigues, S.M., Araújo, C., Coelho, J.P., Pereira, E., Duarte, A.C., 2009. Mercury contamination in the vicinity of a chlor-alkali plant and potential risks to local population. Sci. Total Environ. 407, 2689–2700. https://doi.org/10.1016/j.scitotenv.2008.10.065.
Revis, N.W., Osborne, T.R., Holdsworth, G., Hadden, C., 1989. Distribution of mercury species in soil from a mercury-contaminated site. Water Air Soil Pollut. 45, 105–113. https://doi.org/10.1007/BF00208581.
Rinklebe, J., During, A., Overesch, M., Du Laing, G., Wennrich, R., Stärk, H.-J., Mothes, S., 2010. Dynamics of mercury fluxes and their controlling factors in large Hg-polluted floodplain areas. Environ. Pollut. 158, 308–318. https://doi.org/10.1016/j.envpol.2009.07.001.
Ruzzenenti, M., 2001. Un secolo di cloro e... PCB: storia delle industrie Caffaro di Brescia, Terra-terra. Jaca book ; Alce nero, Milano ([Isola del Piano]).
Shi, J., Liang, L., Jiang, G., Jin, X., 2005. The speciation and bioavailability of mercury in sediments of Haihe River, China. Environ. Int. 31, 357–365. https://doi.org/10.1016/j.envint.2004.08.008.
Skyllberg, U., Qian, J., Frech, W., Xia, K., Bleam, W.F., 2003. Distribution of mercury, methyl mercury and organic sulphur species in soil, soil solution and stream of a boreal forest catchment. Biogeochemistry 64, 53–76. https://doi.org/10.1023/A:1024904502633.
Terzaghi, E., Morselli, M., Zanardini, E., Morosini, C., Raspa, G., Di Guardo, A., 2018a. Improving the SoilPlusVeg model to evaluate rhizoremediation and PCB fate in contaminated soils. Environ. Pollut. 241, 1138–1145. https://doi.org/10.1016/j.envpol.2018.06.039.
Terzaghi, E., Vergani, L., Mapelli, F., Borin, S., Raspa, G., Zanardini, E., Morosini, C., Anelli, S., Nastasio, P., Sale, V.M., Armiraglio, S., Di Guardo, A., 2019. Rhizoremediation of weathered PCBs in a heavily contaminated agricultural soil: results of a biostimulation trial in semi field conditions. Sci. Total Environ. 686, 484–496. https://doi.org/10.1016/j.scitotenv.2019.05.458.
Terzaghi, E., Zanardini, E., Morosini, C., Raspa, G., Borin, S., Mapelli, F., Vergani, L., Di Guardo, A., 2018b. Rhizoremediation half-lives of PCBs: role of congener composition, organic carbon forms, bioavailability, microbial activity, plant species and soil conditions, on the prediction of fate and persistence in soil. Sci. Total Environ. 612, 544–560. https://doi.org/10.1016/j.scitotenv.2017.08.189.
Tsiros, I.X., Ambrose, R.B., 1999. An environmental simulation model for transport and fate of mercury in small rural catchments. Chemosphere 39, 477–492. https://doi.org/10.1016/S0045-6535(98)00601-8.
US EPA, 2016. Definition and Procedure for the Determination of the Method Detection Limit. Revision 2 (No. EPA 821-R-16-006). U.S. Environmental Protection Agency, Office of Water.
US EPA, 2002. U.S. EPA Method 1631, Revision E: Mercury in Water by Oxidation, Purge and Trap, and Cold Vapor Atomic FluorescenceSpectrometry [WWW Document]. https://nepis.epa.gov/. accessed 3.18.21.
US EPA, O., 2007a. U.S. EPA Method 3051A: Microwave Assisted Acid Digestion of Sediments, Sludges, and Oils [WWW Document]. US EPA. https://www.epa.gov/esam/us-epa-method-3051a-microwave-assisted-acid-digestion-sediments-sludges-and-oils. accessed 3.18.21.
US EPA O., 2007b. U.S. EPA Method 6020A: Inductively Coupled Plasma - Mass Spectrometry [WWW Document]. URL /homeland-security-research/epa-method-6020a-sw-846-inductively-coupled-plasma-mass-spectrometry (accessed 3.18.21).
Vergani, L., Mapelli, F., Zanardini, E., Terzaghi, E., Di Guardo, A., Morosini, C., Raspa, G., Borin, S., 2017. Phyto-rhizoremediation of polychlorinated biphenyl contaminated soils: an outlook on plant-microbe beneficial interactions. Sci. Total Environ. 575, 1395–1406. https://doi.org/10.1016/j.scitotenv.2016.09.218.
Wang, J., Feng, X., Anderson, C.W.N., Qiu, G., Ping, L., Bao, Z., 2011. Ammonium thiosulphate enhanced phytoextraction from mercury contaminated soil – results from a greenhouse study. J. Hazard Mater. 186, 119–127. https://doi.org/10.1016/j.jhazmat.2010.10.097.
Wang, J., Feng, X., Anderson, C.W.N., Xing, Y., Shang, L., 2012. Remediation of mercury contaminated sites – a review. J. Hazard Mater. 221–222, 1–18. https://doi.org/10.1016/j.jhazmat.2012.04.035.
Yang, J., Takaoka, M., Sano, A., Matsuyama, A., Yanase, R., 2018. Vertical distribution of total mercury and mercury methylation in a landfill site in Japan. Int. J. Environ. Res. Publ. Health 15, 1252. https://doi.org/10.3390/ijerph15061252.
Yediler, A., Grill, P., Sun, T., Kettrup, A., 1994. Fate of heavy metals in a land treatment system irrigated with municipal wastewater. Chemosphere 28, 375–381. https://doi.org/10.1016/0045-6535(94)90134-1.
Yin, R., Gu, C., Feng, X., Hurley, J.P., Krabbenhoft, D.P., Lepak, R.F., Zhu, W., Zheng, L., Hu, T., 2016. Distribution and geochemical speciation of soil mercury in Wanshan Hg mine: effects of cultivation. Geoderma 272, 32–38. https://doi.org/10.1016/j.geoderma.2016.03.003.
Zhang, Y., Wang, M., Huang, B., Akhtar, M.S., Hu, W., Xie, E., 2018. Soil mercury accumulation, spatial distribution and its source identification in an industrial area of the Yangtze Delta, China. Ecotoxicol. Environ. Saf. 163, 230–237. https://doi.org/10.1016/j.ecoenv.2018.07.055.